ChemComm

COMMUNICATION

View Article Online
View Journal | View Issue

Cite this: *Chem. Commun.*, 2015, **51**, 13523

Received 28th June 2015,
Accepted 15th July 2015

DOI: 10.1039/c5cc05301c

www.rsc.org/chemcomm

Highly transparent and flexible polyimide/ZrO_2 nanocomposite optical films with a tunable refractive index and Abbe number†

Chia-Liang Tsai and Guey-Sheng Liou*

In this study, novel thermally stable zirconia-containing polyimides (PI/ZrO_2) with excellent optical properties have been prepared successfully. The obtained flexible PI/ZrO_2 hybrid films revealed excellent optical transparency, a tunable refractive index and an Abbe number up to 1.804 and 32.18, respectively, which are crucial for optical devices. In addition, the PI/ZrO_2 hybrid films also exhibit a higher Abbe number and transparency in the visible light region due to a larger energy band gap of ZrO_2 than the corresponding PI/TiO_2 system.

High refractive index polymers have been widely proposed in recent years for the advanced optoelectronic applications. In addition to the basic parameter of the refractive index, other properties such as birefringence, Abbe number, optical transparency, processability, and thermal stability are also important and have to be taken into consideration for practical optical applications. Therefore, it is a crucial and on-going issue to achieve the requirements mentioned above.[1] Polyimides (PIs) are the most promising candidates for optical device applications owing to their excellent thermal stability, chemical resistance, and outstanding mechanical properties. In addition, by molecular architecture design and synthesis, polyimides with good processability and well-balanced optical properties could be simultaneously obtained, making the polyimide optical materials an intensively investigated research area.[2] Fluorene and its derivatives with a bulky and rigid structure are well-known candidates as optical materials when incorporated into a polymer backbone, and could reduce the intermolecular interaction and packing density of the PI chains to enhance the transparency and processability of the corresponding PIs.[3]

Recently, polymer–inorganic hybrid materials have attracted a great deal of attention owing to the outstanding combinations of mechanical, thermal, magnetic, optical, electronic, and optoelectronic properties when compared with individual polymer or inorganic components.[4–6] For optical material applications, the inorganic domains must be controlled to be less than 40 nm in diameter for reducing scattering loss and maintaining the optical transparency.[7] Chemical bonding approaches based on *in situ* sol–gel reaction made it possible to overcome the agglomeration phenomenon of inorganic nanoparticles by manipulating the organic/inorganic interactions at various molecular and nanometer length scales, and the polyimide/titania (PI/TiO_2) hybrids with a high refractive index could be achieved by increasing the TiO_2 content in our previous studies.[8] However, the optical transparency of the obtained PI/TiO_2 hybrid films reduced dramatically at a wavelength of around 400 nm attributed to the low band gap of TiO_2 (3.2 eV), resulting in pale yellow color of the hybrid films. Besides, the Abbe number of the PI/TiO_2 hybrid films also decreased with increasing TiO_2 content. Thus, choosing species of inorganic materials in the hybrid system for enhancing the refractive index without sacrificing the Abbe number and optical transparency in the visible light region is an important issue.

Zirconia (ZrO_2) has excellent combination of optical properties, such as a high refraction index, Abbe number, and transparency on a broad spectral range due to the large band gap of ZrO_2 in the range 5.0–5.85 eV.[9–11] Therefore, a facile *in situ* sol–gel approach for obtaining optically transparent polyimide/zirconia (PI/ZrO_2) hybrids was used in this study. The pendent hydroxyl groups in PI chains could provide the organic–inorganic bonding sites with zirconium butoxide ($Zr(OBu)_4$) to obtain PI/ZrO_2 hybrid films with different ZrO_2 contents for advanced optical applications.

FOH-6FPI and **FOH-CHPI** synthesized by the one-step polycondensation starting from hydroxyl-substituted diamine monomers F-DA, aromatic tetracarboxylic dianhydrides 6FDA and alicyclic dianhydrides CHDA in the presence of a catalytic amount of isoquinoline at 170–180 °C, and the fabrication procedure of hybrid films from **FOH-6FPI**, **FOH-CHPI** and zirconia precursor are depicted in Scheme 1, respectively. The flexible, transparent, and homogeneous PI–nano-zirconia hybrid optical films with different zirconia contents (up to 50 wt%)

Functional Polymeric Materials Laboratory, Institute of Polymer Science and Engineering, National Taiwan University, 1 Roosevelt Road, 4th Sec., Taipei 10617, Taiwan. E-mail: gsliou@ntu.edu.tw; Fax: +886-2-33665237; Tel: +886-2-33665070

† Electronic supplementary information (ESI) available: Experimental section, table displaying basic properties and figure showing basic properties of hybrids. See DOI: 10.1039/c5cc05301c

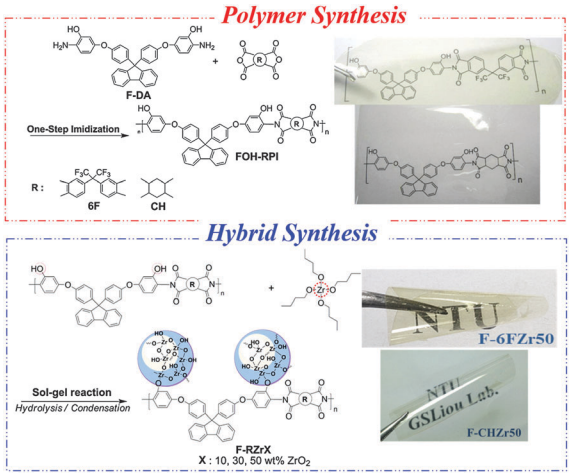

Scheme 1 Synthesis and structures of the poly(*o*-hydroxy-imide)s and preparation of PI/zirconia hybrids.

could be successfully prepared, which are also shown in Scheme 1. The detailed synthetic procedure and basic properties are described in the ESI.†

Thermal behaviors of the obtained PI/ZrO_2 (**F-6FZr*X*** and **F-CHZr*X***) and PI/TiO_2 (**F-6FTi*X***) hybrids evaluated by TGA and TMA are summarized in Table S2 (ESI†). The typical TGA curves (Fig. S3, ESI†) of **F-6FZr*X*** revealed excellent thermal stability up to 400 °C both in nitrogen and air, and carbonized residue (char yield) increased with increasing zirconia content. The zirconia contents in the hybrid materials estimated based on the char yields under air flow matched with the theoretical calculation and ensured successful incorporation of the zirconia. The typical TMA thermograms for **FOH-6FPI** and the corresponding hybrid materials revealed that the glass transition temperature increased from 257 °C to 358 °C with increasing zirconia content (Fig. S4, ESI†). Meanwhile, the coefficient of thermal expansion (CTE) of the pure PIs, PI/ZrO_2, and PI/TiO_2 hybrid films is summarized in Table S2 (ESI†), and the reinforced hybrids revealed much lower CTE values than pristine PIs, and decreased upon increasing the volume fraction of inorganic reinforcement.

The UV-visible (UV-vis) transmission spectra of the TiO_2 and ZrO_2 hybrid thick (thickness: 19 ± 3 μm) and thin (thickness: 500–600 nm) films were investigated, and the results are summarized in Fig. 1 and Table 1. These well-dispersed PI/ZrO_2 thin hybrid films revealed excellent optical transparency with lower cutoff wavelengths in the UV region. The cutoff wavelength of the PI/TiO_2 hybrid materials red-shifted upon increasing the titania content, and the transparency decreased significantly at a wavelength of 450 nm even when the size of the titania domain is less than 10 nm.[12]

In addition, the cutoff wavelength of the PI/ZrO_2 hybrid films also red-shifted with increasing zirconia content. Generally, the overall optical absorbance of a hybrid film could be enhanced by not only its absorption coefficient but also the path length of light within materials. The optical thickness is to scatter incident light, and scattering always occurs when the refractive index of

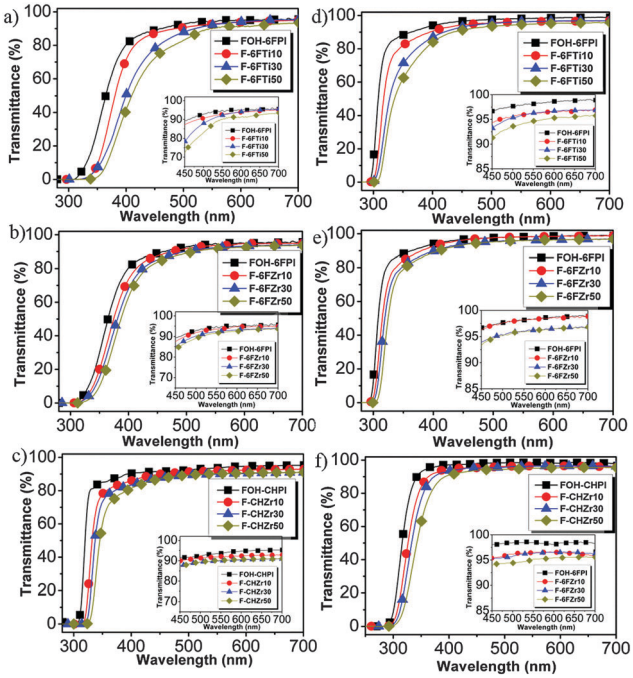

Fig. 1 Optical transmission spectra of **F-6FTi*X***, **F-6FZr*X*** and **F-CHZr*X*** hybrid thick films (a), (b), (c) (thickness: 19 ± 3 μm); and thin films (d), (e), (f) (thickness: 500–600 nm). The inset figure shows the transmission spectra of hybrid thick and thin films in 450–700 nm of wavelength.

Table 1 Optical properties of the hybrid films with ZrO_2 and TiO_2

	Optical properties					
Index	λ_0[a] (nm)	T_{400}[b] (%)	T_{450}[b] (%)	n[c]	Δn[d]	V_d[e]
FOH-6FPI	292/312	94/83	96/90	1.632	0.0058	19.44
F-6FZr10	295/320	92/80	96/88	1.673	0.0071	20.65
F-6FZr30	298/322	90/76	94/85	1.735	0.0096	28.23
F-6FZr50	303/323	89/72	94/84	1.804	0.0115	32.18
100 wt% ZrO_2	—	95[f]	96[f]	1.897	0.0278	38.20
F-6FTi10	295/327	90/76	94/87	1.682	0.0073	19.54
F-6FTi30	298/327	87/58	93/79	1.742	0.0092	19.02
F-6FTi50	306/340	83/49	91/73	1.817	0.0108	19.25
100 wt% TiO_2	—	84[g]	89[g]	1.983	0.0398	18.32
FOH-CHPI	287/308	97/90	97/92	1.635	0.0063	22.70
F-CHZr10	295/316	94/86	95/90	1.679	0.0075	21.43
F-CHZr30	298/319	93/84	95/88	1.727	0.0099	25.73
F-CHZr50	303/321	91/82	93/88	1.795	0.0118	30.28

[a] The cutoff wavelength (λ_0) from the UV-vis transmission spectra of polymer thin films/thick films (thickness: 500–600 nm/19 ± 2 μm). [b] Transmittance of polymer thin films/thick films (thickness: 500–600 nm/19 ± 2 μm) at 400 and 450 nm. [c] Refractive index at 633 nm obtained using an ellipsometer. [d] The in-plane/out-of-plane birefringence (Δn) calculated as $\Delta n = n_{TE} - n_{TM}$ was measured using a prism coupler. [e] Abbe's number is given by $V_d = n_{587.56} - 1/n_{486.1} - n_{656}$. [f] Transmittance of 100 wt% ZrO_2 thin films (thickness: 100 ± 15 nm) at 400 and 450 nm. [g] Transmittance of 100 wt% TiO_2 thin films (thickness: 100 ± 15 nm) at 400 and 450 nm (100 wt% ZrO_2 and TiO_2 were synthesized from $Zr(OBu)_4$ and $Ti(OBu)_4$ by sol–gel reaction heated to 300 °C, respectively).

medium is locally perturbed which increases with increasing content of ZrO_2 in the PI matrix. Because the particle size of ZrO_2 is less than 10 nm, the red-shift phenomenon could be

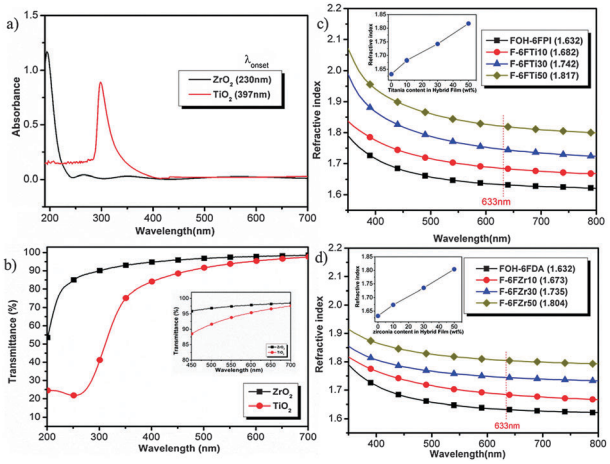

Fig. 2 (a) UV-visible absorption spectra of ZrO_2 and TiO_2 (thickness: 200–300 nm), (b) optical transmission spectrum of ZrO_2 and TiO_2 thin films (thickness: 100 ± 15 nm) (100 wt% ZrO_2 and TiO_2 were synthesized from $Zr(OBu)_4$ and $Ti(OBu)_4$ by sol–gel reaction heated to 300 °C, respectively). The inset figure shows the transmission spectra of ZrO_2 and TiO_2 in 450–700 nm of wavelength. Variation of the refractive index of the (c) **F-6FTi*X***, (d) **F-6FZr*X*** hybrid films with wavelength. The inset figure shows the variation of the refractive index at 633 nm with different titania and ziconia content.

ascribed to the slight variation in the particle size with an increase of the zirconia amount in the hybrid film as a similar trend of the titania hybrid system.[12] Moreover, the transparency exhibited by the obtained zirconia hybrid film at 400 nm is very slightly reduced, which could be ascribed to the much shorter absorption wavelength edge of ZrO_2 (230 nm) than that of TiO_2 (400 nm) because the energy band gap of ZrO_2 (5.0–5.85 eV) is comparatively larger than TiO_2 (3.2 eV) as shown in Fig. 2(a).

In addition, the 100 wt% ZrO_2 thin film also exhibits superior optical transparency (96%) at a wavelength of 450 nm than the 100 wt% TiO_2 thin film (88%) (Fig. 2(b)). Thus, these results demonstrate that the PI/ZrO_2 hybrid system is an excellent alternative for high-performance optical materials in terms of transparency.

Furthermore, semi-aromatic PIs derived from alicyclic dianhydride or diamine have higher transparency due to the absence of intra- and inter-molecular charge-transfer (CT) interactions.[8c] Therefore, the incorporation of alicyclic units into **FOH-CHPI** results in higher transparency in the UV-visible region than the corresponding aromatic PI (**FOH-6FPI**), and the zirconia-containing **FOH-CHPI** hybrid films (**F-CHZr*X***) exhibited higher transparency than the **F-6FZr*X*** hybrid system, the results are summarized in Fig. 1 and Table 1.

The refractive index dispersion in the range of 350–800 nm and the refractive index at 633 nm of the obtained films with different titania and zirconia contents, respectively, are shown in Fig. 2(c) and (d) and the corresponding inset figures, respectively. The refractive index increased linearly with increasing zirconia contents, suggesting that the Zr–OH groups of the hydrolyzed precursors condensed progressively to form the Zr–O–Zr structures and enhance the refractive index. Furthermore, the ZrO_2 hybrid system not only could increase the refractive index but also

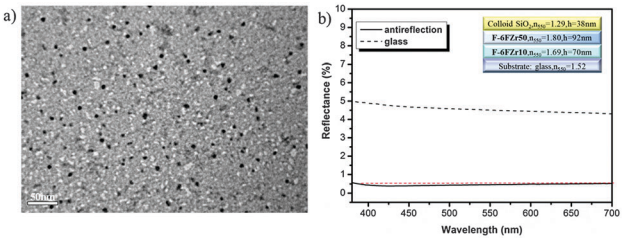

Fig. 3 (a) TEM image of the hybrid film of **F-6FZr50**; (b) variation of the reflectance of the glass slide with wavelength by three-layer antireflection coating.

effectively improves the Abbe number, which is attributed to ZrO_2 with a higher Abbe number than TiO_2, and the results are also summarized in Table 1.

Combining the issues of thickness, flexibility, and optical transparency, the PI/ZrO_2 hybrid optical thick film **F-6FZr50** (19 ± 3 μm in thickness) showed higher optical transparency than the corresponding PI/TiO_2 hybrid film.

The TEM image of the **F-6FZr50** film is shown in Fig. 3(a), and the black spots uniformly dispersed in the hybrid film are ZrO_2 particles with an average domain size of about 6 nm. The resulting ZrO_2 in the hybrid film is amorphous as shown in Fig. S5 (ESI†) because an annealing temperature of 300 °C could only be applied (the crystallization temperature of ZrO_2 should be higher than 500 °C as demonstrated in Fig. S6, ESI†).

The structure of the three layer anti-reflective coating on the glass substrate and the reflectance spectra are depicted in Fig. 3(b), and the glass substrate exhibited a refractive index (n = 1.52) higher than air (n = 1.0) and revealed an average reflectance of about 4.5% in the visible light range. The reflectance could be reduced significantly *via* the three-layer antireflection structure consisting of colloid SiO_2, **F-6FZr50**, and **F-6FZr10** for the first, second, and third layer with a thickness and refractive index of 38 nm (1.29), 92 nm (1.80), and 70 nm (1.69), respectively. The reflectance of the glass substrate with anti-reflection coatings was less than 0.5% in the visible range (400–700 nm), demonstrating the great potential of the highly transparent PI/ZrO_2 hybrid films for optical applications.

In conclusion, the colorless and flexible polyimides were readily prepared from the fluorene-containing diamine with commercial dianhydrides 6FDA and CHDA, respectively. These polyimides with pendent hydroxyl groups could provide the organic–inorganic bonding sites for the formation of nanoscale zirconia by sol–gel reaction. The refractive index and the Abbe number of the resulting PI/ZrO_2 hybrid system are tunable and up to 1.804 and 32.18, respectively, upon increasing the zirconia content. In addition, these PI/ZrO_2 hybrid films also revealed much higher optical transparency than the corresponding PI/TiO_2 system due to the large band gap of ZrO_2. Furthermore, three-layer anti-reflective coating based on the hybrid films exhibited a reflectance of less than 0.5% in the visible light region, suggesting the great potential of these novel PI/ZrO_2 hybrid films for advanced optical applications.

The authors gratefully acknowledge the Ministry of Science and Technology of Taiwan for the financial support.

Notes and references

1 (*a*) T. Nakamura, H. Fujii, N. Juni and N. Tsutsumi, *Opt. Rev.*, 2006, **13**, 104; (*b*) D. W. Mosley, K. Auld, D. Conner, J. Gregory, X. Q. Liu, A. Pedicini, D. Thorsen, M. Wills, G. Khanarian and E. S. Simon, *Proc. SPIE*, 2008, **6910**, 691017; (*c*) K. C. Krogman, T. Druffel and M. K. Sunkara, *Nanotechnology*, 2005, **16**, S338; (*d*) R. D. Allen, G. M. Wallraff, D. C. Hofer and R. R. Kunz, *IBM J. Res. Dev.*, 1997, **41**, 95.

2 (*a*) J. G. Liu and M. Ueda, *J. Mater. Chem.*, 2009, **19**, 8907; (*b*) Y. Suzuki, T. Higashihara, S. Ando and M. Ueda, *Macromolecules*, 2012, **45**, 3402; (*c*) C. A. Terraza, J. G. Liu, Y. Nakamura, Y. Shibasaki, S. Ando and M. Ueda, *J. Polym. Sci., Part A: Polym. Chem.*, 2008, **46**, 1510; (*d*) N. H. You, Y. Suzuki, D. Yorifuji, S. Ando and M. Ueda, *Macromolecules*, 2008, **41**, 6361; (*e*) J. G. Liu, Y. Nakamura, Y. Shibasaki, S. Ando and M. Ueda, *Macromolecules*, 2007, **40**, 4614; (*f*) J. G. Liu, Y. Nakamura, Y. Suzuki, Y. Shibasaki, S. Ando and M. Ueda, *Macromolecules*, 2007, **40**, 7902; (*g*) N. H. You, T. Higashihara, S. Yasuo, S. Ando and M. Ueda, *Polym. Chem.*, 2010, **1**, 480; (*h*) N. H. You, T. Higashihara, S. Ando and M. Ueda, *J. Polym. Sci., Part A: Polym. Chem.*, 2010, **48**, 656; (*i*) N. Fukuzaki, T. Higashihara, S. Ando and M. Ueda, *Macromolecule*, 2010, **43**, 1836.

3 C. A. Terraza, J. G. Liu, Y. Nakamura, Y. Shibasaki, S. Ando and M. Ueda, *J. Polym. Sci., Part A: Polym. Chem.*, 2008, **46**, 1510.

4 (*a*) L. L. Beecroft and C. K. Ober, *Chem. Mater.*, 1997, **9**, 1302; (*b*) C. Sanchez, B. Lebeau, F. Chaput and J. P. Boilot, *Adv. Mater.*, 2003, **15**, 1969; (*c*) R. M. Laine, *J. Mater. Chem.*, 2005, **15**, 3725; (*d*) A. Zelcer, B. Donnio, C. Bourgogne, F. D. Cukiernik and D. Guillon, *Chem. Mater.*, 2007, **19**, 1992; (*e*) Z. Zhou, A. W. Franz, M. Hartmann, A. Seifert, T. J. J. Muller and W. R. Thiel, *Chem. Mater.*, 2008, **20**, 4986; (*f*) F. Pereira, K. Valle, P. Belleville, A. Morin, S. Lambert and C. Sanchez, *Chem. Mater.*, 2008, **20**, 1710; (*g*) Y. Y. Lin, C. W. Chen, T. H. Chu, W. F. Su, C. C. Lin, C. H. Ku, J. J. Wu and C. H. Chen, *J. Mater. Chem.*, 2007, **17**, 4571; (*h*) J. S. Kim, S. C. Yang and B. S. Bae, *Chem. Mater.*, 2010, **22**, 3549; (*i*) P. Xue, J. Wang, Y. Bao, Q. Li and C. Wuac, *New J. Chem.*, 2012, **36**, 903; (*j*) S. C. Yang, S. Y. Kwak, J. H. Jin, J. S. Kim, Y. Choi, K. W. Paikb and B. S. Bae, *J. Mater. Chem.*, 2012, **22**, 8874.

5 *Functional Hybrid Materials*, ed. P. Gomez-Romero and C. Sanchez, Wiley-VCH, Weinheim, 2004.

6 G. Kickelbick, *Hybrid Materials: Synthesis, Characterization, and Applications*, Wiley-VCH, Weinheim, 2007.

7 H. Althues, J. Henle and S. Kaskel, *Chem. Soc. Rev.*, 2007, **36**, 1454.

8 (*a*) G. S. Liou, P. H. Lin, H. J. Yen, Y. Y. Yu, T. W. Tsai and W. C. Chen, *J. Mater. Chem.*, 2010, **20**, 531; (*b*) C. L. Tsai, H. J. Yen, W. C. Chen and G. S. Liou, *J. Mater. Chem.*, 2012, **22**, 17236; (*c*) H. J. Yen, C. L. Tsai, P. H. Wang, J. J. Lin and G. S. Liou, *RSC Adv.*, 2013, **3**, 17048.

9 (*a*) M. Zelner, H. Minti, R. Reisfeld, H. Cohen and R. Tenne, *Chem. Mater.*, 1997, **9**, 2541; (*b*) A. Sashchiuk, E. Lifshitz, R. Reisfeld, T. Saraidarov, M. Zelner and A. Willenz, *J. Sol-Gel Sci. Technol.*, 2002, **24**, 31; (*c*) M. T. Wang, T. H. Wang and J. Lee, *Microelectron. Reliab.*, 2005, **45**, 969.

10 H. D. E. Harrison, N. T. McLamed and E. C. Subbaro, *J. Electrochem. Soc.*, 1963, **110**, 23.

11 (*a*) A. Emeline, G. V. Kataeva, A. S. Litke, A. V. Rudakova and N. Serpone, *Langmuir*, 1998, **14**, 5011; (*b*) R. Bensaha and H. Bensouyad, *Heat Treatment – Conventional and Novel Applications*, INTECH, 2012, ch. 10, p. 207.

12 M. Anpo, T. Shima, S. Kodama and Y. Kubokawa, *J. Phys. Chem.*, 1987, **91**, 4305.

